Pareto Optimization of Power and Efficiency for Lunar Rover Wireless Power Transfer System with Multi-layer Insulation

Mingyang Chen [1], Bingcheng Ji [1], Katsuhiro Hata [2], Takehiro Imura[3], Hiroshi Fujimoto[1], Yoichi Hori[1]
Sayuri Honda[4], Shuhei Shimada[4] and Osamu Kawasaki[4]

1 Department of Advanced Energy, Graduate School of Frontier Sciences, The University of Tokyo

2 Department of Informatics and Electronics, Institute of Industrial Science, The University of Tokyo

3 Department of Electrical Engineering, Tokyo University of Science

4 Research Unit I, R&D Directorate, Japan Aerospace Exploration Agency

E-mail: chin.meiyou19@ae.k.u-tokyo.ac.jp

Abstract The MLI materials employed in the lunar rover WPT system can achieve the rover body side thermal insulation to reduce the thermal dissipation, and on the other hand, it also reduces the WPT power transfer efficiency under working conditions. In order to reduce the negative impact, the optimal frequency of the WPT system with MLI materials is investigated based on the coil property variation at different frequencies and equivalent power transfer model. Then, to conduct the maximum efficiency and power energy transfer, the Pareto Front of the optimal frequency is analyzed.

Keyword lunar rover, multi-objective optimization, wireless power transfer, multi-layer insulation, frequency optimization

1. Introduction

Lunar rover is a kind of vehicle powered by photovoltaic panels, and it is used in lunar surface exploration [1]. Between lunar day and night, there is an intense variation in the temperature. In order to protect the lunar rover from the extreme temperature on the moon, the multi-layer insulation (MLI) materials are used to cover the surface of the lunar rover [2]. MLI materials consists of layers of aluminum foils, with each layer thickness as 100 nm, and are used for thermal isolation in space exploration areas. However, there is still some part of the lunar rover cannot be covered by MLI, for example the PV panels and the wire connecting to the lunar rover. As a result, the heat leakage from the wire and the PV panels cannot be ignored. Novel structures with wireless power transfer (WPT) replacing the wire which connects the PV panels and the lunar rover's body is proposed in recent research in order to avoid the heat leakage from the wire [3][4]. In the proposed structure, there will be MLI materials placed between transmitter and receiver side coils. Because MLI are metal materials, the eddy current will be generated inside the MLI by the alternating magnetic field. This will result in a loss of the total transferred power, reducing the efficiency of WPT system.

Because the eddy current loss is highly dependent on the operating frequency [5], the frequency selection is necessary to compensate the influence of MLI materials. For WPT systems on the earth, there are restrictions for the operating frequency selection. Generally, the operating frequency of the WPT systems on electrical vehicles is always around 85kHz by SAE, but for lunar rovers there is no such restriction indicating a wide range of frequency can be selected. Based on the previous research, the frequency optimization for WPT system on lunar rover is conducted in order to improve the efficiency and power of lunar rover WPT systems.

Some of the previous research about WPT frequency optimization usually focus on the copper loss of the coils and power electronics losses [6][7]. Others discussing frequency selection in underwater WPT systems also take eddy current loss into consideration [5][8]. Losses are analyzed precisely in these papers, but only the efficiency is discussed as optimization target. Multi-objective optimization for WPT systems is conducted in other research [9], but the optimization object is not frequency. And because there is no MLI materials in these researches, their conclusion cannot be used for lunar rover WPT systems directly.

In this paper, a multi-objective optimization considering both efficiency and power is presented based on the measurement data of coils. With applying pareto optimization to frequency selection, the influence of the eddy current between the coils is discussed, and the recommended frequency range for higher efficiency and power for different position of MLI materials is presented.

2. Circuit Analysis and Objective Function Definition

Pareto front is a set of feasible solutions, which are presented for different cases. On the Pareto front, the increase of one of the objective functions will result in a decrease of the other objective functions. The objective functions in this paper are the WPT efficiency in the efficiency tracking mode and a function representing the transferred power under the power

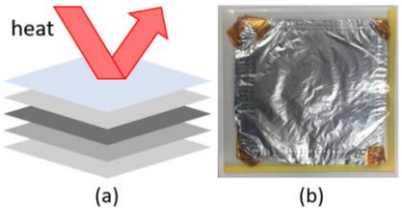

Fig. 1. (a) Profile of MLI materials. (b) MLI materials.

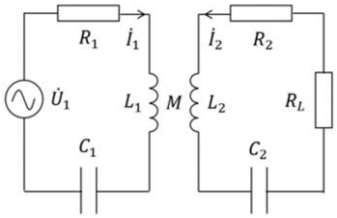

Fig. 2. SS topology of WPT circuit.

tracking mode.

Although the operating condition of these two modes are different, which means we cannot achieve these two modes simultaneously, we still consider the frequency with higher power and efficiency more valuable, because it has a better performance at both modes. By adopting the frequency range in this paper, both theoretical highest efficiency and power of the WPT system will be optimized.

In this paper, for the WPT system, the SS topology is employed, as shown in Fig. 2. The circuit equations are:

$$\begin{cases} \left(R_1 + j\omega L_1 + \frac{1}{j\omega C_1}\right) \cdot \dot{I}_1 + j\omega M \cdot \dot{I}_2 = \dot{U}_1 \\ j\omega M \cdot \dot{I}_1 + \left(R_2 + R_L + j\omega L_2 + \frac{1}{j\omega C_2}\right) \cdot \dot{I}_2 = 0 \end{cases} \quad (1)$$

Where R_1,R_2;L_1,L_2;C_1,C_2 represent the resistances, self-inductances and capacitances of the first and secondary side, respectively. $\dot{U}_1$ is the input voltage; $\dot{I}_1$ and $\dot{I}_2$ are the first and secondary side currents, respectively. ω represents the operating angle frequency and M is the mutual inductance. R_L is the load resistance.

At the resonance frequency, the inductance and capacitance cancels with each other:

$$\omega L_1 = \frac{1}{\omega C_1}, \omega L_2 = \frac{1}{\omega C_2} \quad (2)$$

The efficiency can be derived as:

$$\eta = \frac{\omega^2 M^2 R_L}{(R_2+R_L)(R_1R_2+R_1R_L+\omega^2M^2)} \quad (3)$$

$$R_L = R_{\eta max} = \sqrt{R_2\left(\frac{\omega^2M^2}{R_1} + R_2\right)} \quad (4)$$

Where the $R_{\eta max}$ is the equivalent resistance at the maximum efficiency.

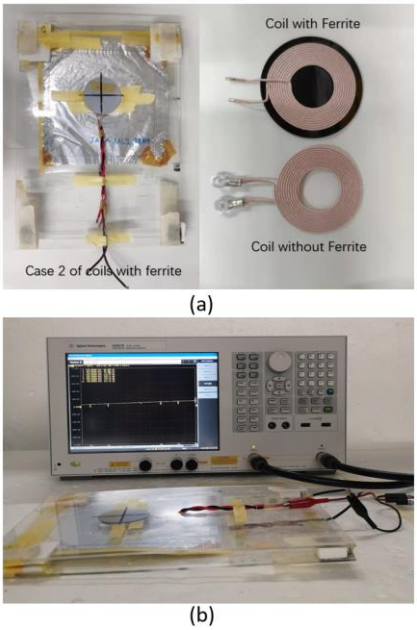

Fig. 3. (a) Employed coils structure (b) Experiment platform.

Substitute (4) into (3), the function of maximum efficiency can be obtained. When the system is fixed, the maximum efficiency is a function of frequency, which is selected as the first objective function. Similarly, when the equivalent resistance of the load equals to:

$$R_{Pmax} = \frac{(\omega M)^2}{R_1} + R_2 \quad (5)$$

R_{Pmax} is the equivalent load resistance at the maximum power. The maximum power of the system is:

$$P_{max} = \frac{1}{4R_1\left(1+\frac{R_1R_2}{(\omega M)^2}\right)}\dot{U}_1^{\,2} = k_p\dot{U}_1^{\,2} \quad (6)$$

Because the maximum power depends on the first side voltage, the factor k_p independent from the voltage is chosen as the second objective function. With a unit of Ω^{-1}. The reason of ignoring primary side voltage is that the primary side voltage and current are determined by the maximum power tracking of the photovoltaic panels, in other words, they are determined by the property of the PV panels and independent from frequency.

$$k_p = \frac{1}{4R_1\left(1+\frac{R_1R_2}{(\omega M)^2}\right)} \quad (7)$$

3. Optimization Methodology

The employed Pareto optimization is conduced based on the Chebyshev matric method with following process. Firstly, the $-\eta$ and $-k_p$ are regarded as the horizontal and vertical coordinates of a vector Z, and all the Z vectors are plotted in the coordinate system.

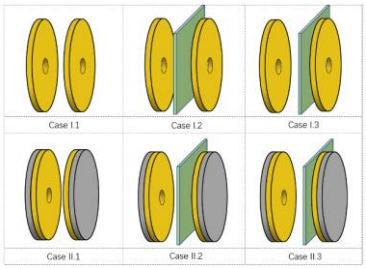

Fig. 4. Three cases of MLI and ferrite position.

Tab. 1. Coil properties

Coils	K	Gap(mm)	L_1(μH)	L_2(μH)
I	0.28	10	3.95	3.96
II	0.40	10	7.03	7.03

Tab. 2. Optimal Frequencies for efficiency (kHz)

Cases	1	2	3
I	699	417	403
II	455	250	220

Then, the weighted Chebyshev distance between Z and an ideal vector Z^* is calculated. The frequency at the lowest weighted distance will be the feasible solution at this weighted number. By changing the weighed number, a set of feasible solutions can be obtained.

3.1. Ideal Vector Setting

Because the ideal efficiency is 100%, the horizontal coordinate of Z^* is set to be -1. According to the equation of $-k_p$, because the resistance always increases more rapidly with respect to the frequency than the frequency itself, k_p decreases with respect to the frequency. In this paper, $-k_p{}^*$ is set to be $-5\ \Omega^{-1}$ based on the measurement.

3.2. Constraint Conditions

To make the discussion more practical, the lower limit of secondary current has been taken into consideration. Based on the circuit of section 2, the secondary current equals to:

$$\dot{I}_2 = \frac{j\omega M \dot{U}_1}{R_1(R_2+R_L)+\omega^2 M^2} = k_c \dot{U}_1 \qquad (8)$$

The absolute value of k_c decreases with respect to the frequency. The maximum power tracking mode has the highest output power at the arbitrary frequency, and then the only thing needs to be determined is the lower limit of the current for the efficiency tracking mode. In this paper, $|\dot{I}_2|$ is set not to be less than $|\dot{U}_1| * 0.1$. The purpose is to ensure the lowest load current at efficiency tracking. The frequency range in this paper is 50-700 kHz, because for higher frequencies, the proximity effect of the coils will be relatively higher.

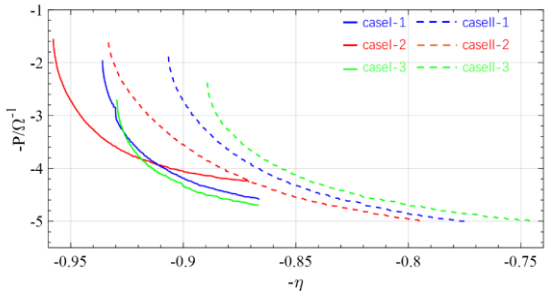

Fig. 5. Pareto Front for 6 cases.

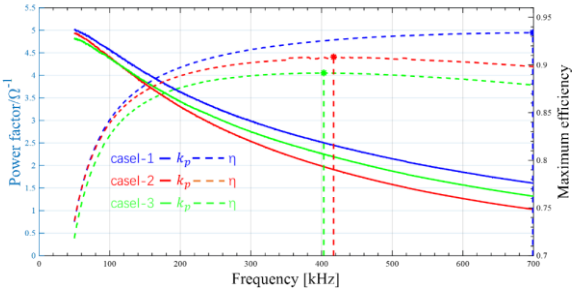

Fig. 6. Efficiency and power with respect to frequency for case I.

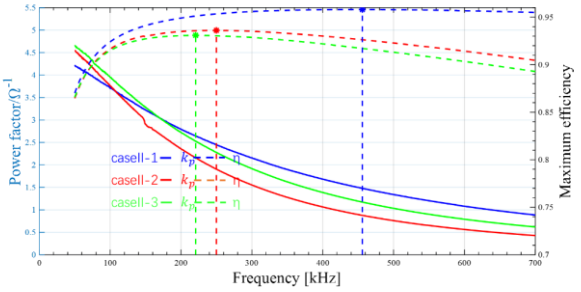

Fig. 7. Efficiency and power with respect to frequency for case II.

While for the lower frequency, the quality factor of coils is usually not sufficient.

Finally, the mathematical expression of the optimization is:

$$\begin{aligned} &min && l(f) = \max\left(w_1(\eta(f)-\eta^*), w_2(P(f)-P^*)\right) \\ &\text{subject to} && |\dot{I}_2(f)| \geq 0.1|\dot{U}_1| \\ & && 50kHz \leq f \leq 700kHz \end{aligned} \qquad (7)$$

4. Experiment and Pareto Optimization

4.1 Experiment Measurement

The employed coil and experiment platform are shown in Fig. 3(a) and (b), respectively. The MLI used in this paper is specially designed with slit on the surface, to reduce the magnetic shielding effect while ensuring the isothermal property. The coils employed are TDK 10K2-A11-6-T170909. The distance between coils is 10 mm. There are three cases of different position for MLI materials. In the first case

there is no MLI. In the second case MLI materials are placed in the middle of the coils. In the third case the MLI materials are placed 1 mm from coil 2, coils with or without ferrite have been measured, as shown in Fig. 4. The measured properties are the AC resistance, self and mutual inductances of the coils.

4.2 Optimization Result

The optimization result has been shown in Fig. 5, calculated by (7) based on the measurement of section 4.1. The Pareto front shows how the theoretical efficiency contracts with theoretical power. It is observed from the optimization result that the range of optimal frequency is from 50 kHz to the frequency at the peak of the efficiency curve. To express the optimization result, efficiency and power factor with respect to each frequency is plotted in Fig. 6 and 7, calculated by (3) to (6). The optimal frequency for maximum efficiency has been shown in Tab. 2, where the optimal frequency is set to be 699 kHz, which may be inaccurate as the efficiency is still increasing with respect to the frequency. Considering the power factor is a decrease function and the efficiency curve is a unimodal curve, the recommended frequency range is the frequency lower than the optimal frequency of efficiency curve.

Comparing the optimal frequency under the presence or absence of ferrite and MLI material, it is concluded that both of them reduces the upper limit of the recommended operating frequency. The reason is that both ferrite and MLI materials can cause intense increase in the coil resistance, which leads to the optimal frequency decrease with respect to the efficiency.

The optimization result can be summarized as follows. Firstly, the operating frequency should be lower than the optimal frequency of the efficiency curve, considering the power factor is decreasing with respect to resonance frequency. Secondly, because the ferrite and MLI reduce the optimal frequency of the efficiency curve, the operating frequency for the system with ferrite or MLI should be selected lower than frequency for systems without ferrite and MLI. The position of MLI also influences the frequency selection, in the cases which MLI is placed apart from the secondary coil at 1 mm, and the optimal frequency is lower than the cases MLI in the middle of two coils.

5. Conclusion

In this paper, multi-objective optimization is conducted for frequency selection in a lunar rover WPT system. Taking MLI material into consideration, efficiency and power function with respect to frequency is shown by the pareto front of maximum efficiency and power functions. The optimization process is presented in details in this paper. From this optimization result, it is referred that the operating frequency choosing for the WPT system should be lower than the optimal frequency of the efficiency curve. And with MLI and ferrite, the operating frequency is always lower than the cases without MLI and ferrite. These conclusions are valuable for the frequency selection of lunar rover WPT systems.

6. References

[1] Hickman, J. Mark, Henry B. Curtis, and Geoffrey A. Landis, “Design consideration for lunar based photovoltaic power systems.” *IEEE Conference on Photovoltaic Specialists. IEEE*, 1990.

[2] J. Jiang, “Multilayer Insulation Materials and Their Application to Spacecrafts.” Aerospace Materials & Technology, vol. 4, pp. 17-25, 2000

[3] B. Ji, K. Hata, T. Imura, Y. Hori, S. Shimada, S. Honda, S. Ichikawa, “Basic Study of Solar Battery Powered Wireless Power Transfer System with MPPT Mode and DC Bus Stabilization for Lunar Rover.” *IECON 2018-44th Annual Conference of the IEEE Industrial Electronics Society. IEEE*, 2018.

[4] T. Imura, and Y. Hori, “Maximizing air gap and efficiency of magnetic resonant coupling for wireless power transfer using equivalent circuit and Neumann formula,” *IEEE Transactions on Industrial Electronics*, vol. 58, no. 10, pp. 4746-4752, 2011

[5] Q. Deng, J. Liu, D. Czarkowski, M. K. Kazimierczuk, M. Bojarski, H. Zhou, W. Hu, “Frequency-dependent resistance of litz-wire square solenoid coils and quality factor optimization for wireless power transfer,” *IEEE Transactions on Industrial Electronics*, vol. 63, no.5, pp. 2825-2837, 2016.

[6] H. Zhou, X. Gao, J. Lai, W. Hu, Q. Deng, D. Zhou, “Natural frequency optimization of wireless power systems on power transmission lines.” *IEEE Access*, vol. 6, pp. 14038-14047, 2018.

[7] Z. Yan, Y. Zhang, T. Kan, F. Lu, K. Zhang, B. Song, C. C. Mi, “Frequency optimization of a loosely coupled underwater wireless power transfer system considering eddy current loss,” *IEEE Transactions on Industrial Electronics*, vol. 66, no. 5, pp. 3468-3476, 2018.

[8] J. Zhou, D. Li, Y. Chen, “Frequency selection of an inductive contactless power transmission system for ocean observing,” *Ocean Engineering*, vol. 60, pp. 175-185, 2013.

[9] R. Bosshard, J. W. Kolar, J. Mühlethaler , I. Stevanović, B. Wunsch, F. Canales, "Modeling and eta-alpha Pareto Optimization of Inductive Power Transfer Coils for Electric Vehicles," *IEEE Journal of Emerging and Selected Topics in Power Electronics*, vol. 3, no.1, pp. 50-64, 2014